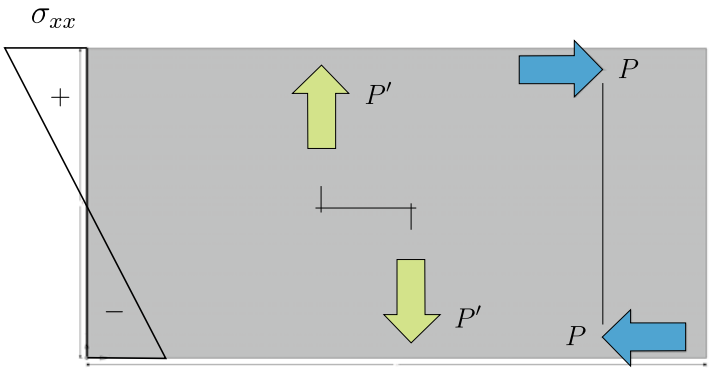

Fig. 6.18 The stresses σ_{xx} remain bounded in these load cases

Remark 6.2 Numerical tests prove that force couples do not produce singular stresses, see Fig. 6.18.

6.8 Standard Situations

But a cantilever plate is not so special. Even at such seemingly harmless points as the reentrant corners of openings in a wall plate, see Fig. 6.19, singularities develop. Normally the meshes are too coarse for the singularities to shine through, but when one really goes all the way in, as in Fig. 6.20, one notices the infinite stresses. In highly stressed mechanical parts as turbine blades such stress singularities can be relevant for the design (stress intensity factors).

6.9 Singularities in Influence Functions

Also influence functions must cope with the singularities on the boundary, because these singularities pollute the FE-solution via an unavoidable "boundary element" mechanism: **Also FE-solutions are potentials**, since they are the superposition of the load with influence functions, see Sect. 9.18.

To understand this, we consider a membrane, which covers an L-shaped opening, see Fig. 6.21. When the wind p presses down on the membrane, the slope of the membrane at the re-entrant corner will be very steep, we may even assume infinite in value, $w_{,x} = \infty$ and $w_{,y} = \infty$, and this means, the shear forces v_x and v_y

$$v_x = H\, w_{,x} \qquad v_y = H\, w_{,y} \qquad H = \text{prestress}\,, \tag{6.19}$$

will be infinite at the re-entrant corner.

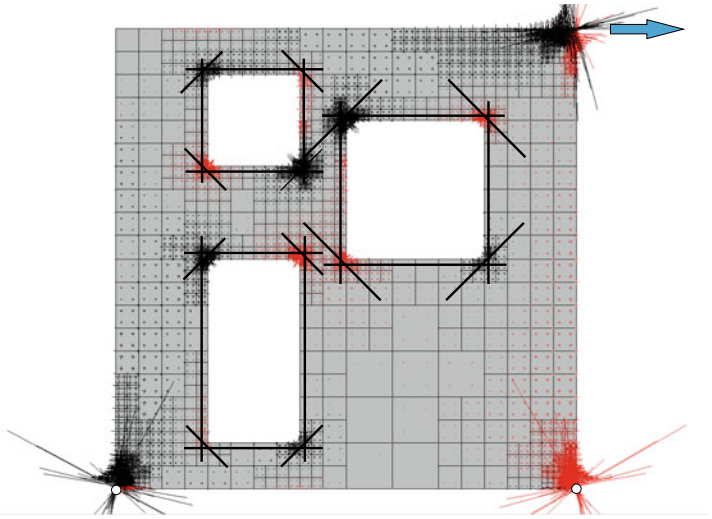

Fig. 6.19 Wall plate with adaptively refined mesh, and constructive reinforcement at the corners

But even in this dramatic situation the influence function for the FE-solution

$$w_h(\boldsymbol{x}) = \int_\Omega G_h(\boldsymbol{y}, \boldsymbol{x})\, p(\boldsymbol{y})\, d\Omega_y\,, \tag{6.20}$$

looks the same and nothing seems to indicate that the kernel $G_h(\boldsymbol{y}, \boldsymbol{x})$ suffers from a singularity at the re-entrant corner. Where do the negative effects of the singularity hide?

We only want to sketch the answer. Readers who are familiar with potential theory or the boundary element method know that the solution of the equation $-\Delta w = p$ can be written as a boundary integral plus a domain integral, see Sect. 9.17,

$$w(\boldsymbol{x}) = \int_\Gamma (g(\boldsymbol{y}, \boldsymbol{x})\, \frac{\partial w}{\partial n}(\boldsymbol{y}) - \frac{\partial g(\boldsymbol{y}, \boldsymbol{x})}{\partial n}\, w(\boldsymbol{y}))\, ds_y + \int_\Omega g(\boldsymbol{y}, \boldsymbol{x})\, p(\boldsymbol{y})\, d\Omega_y\,. \tag{6.21}$$

That is, we can calculate the shape of the surface w via the auxiliary function $g(\boldsymbol{y}, \boldsymbol{x})$ from its boundary values w, and $\partial w/\partial n$ on the edge Γ, and from the way the load p is distributed in the domain Ω.

The function

$$g(\boldsymbol{y}, \boldsymbol{x}) = -\frac{1}{2\,\pi}\, \ln|\boldsymbol{y} - \boldsymbol{x}|\,, \tag{6.22}$$

is called a ***fundamental solution***, since it satisfies the equation $-\Delta g(\boldsymbol{y}, \boldsymbol{x}) = \delta(\boldsymbol{y} - \boldsymbol{x})$.

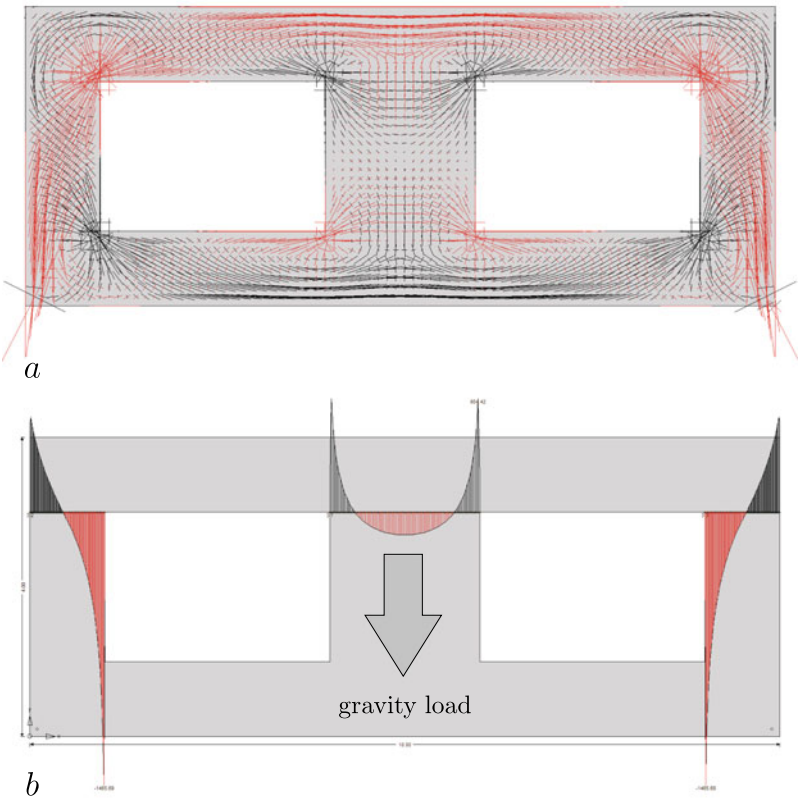

Fig. 6.20 Gravity load in a wall plate on two point supports, **a** principal stresses, **b** stresses σ_{yy} in horizontal sections (BE-solution)

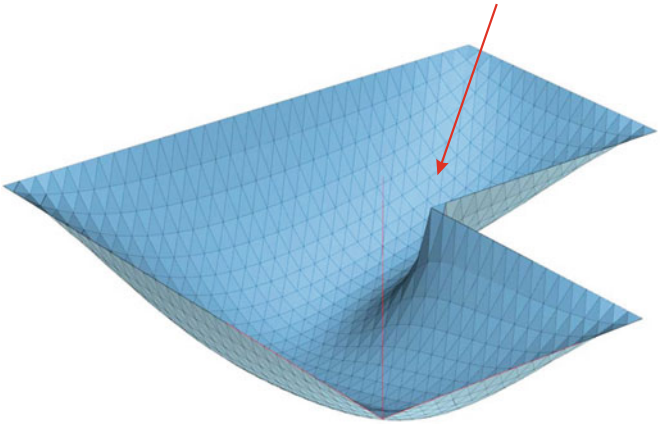

Fig. 6.21 L-shaped membrane under uniform pressure

This integral representation can also be applied to the influence function $G(\boldsymbol{y}, \boldsymbol{x})$. In this situation, the load to which $G(\boldsymbol{y}, \boldsymbol{x})$ corresponds, is a Dirac delta $\delta(\boldsymbol{y} - \boldsymbol{x})$, and since $G(\boldsymbol{y}, \boldsymbol{x})$ is zero on the edge Γ, the equation reduces to

$$\begin{aligned} G(\boldsymbol{y}, \boldsymbol{x}) &= \int_\Gamma [g(\boldsymbol{\xi}, \boldsymbol{y}) \frac{\partial G_h}{\partial n}(\boldsymbol{\xi}, \boldsymbol{x}) - \frac{\partial g(\boldsymbol{\xi}, \boldsymbol{y})}{\partial n} G(\boldsymbol{\xi}, \boldsymbol{x})] \, ds_\xi \\ &\quad + \underbrace{\int_\Omega g(\boldsymbol{\xi}, \boldsymbol{y}) \, \delta(\boldsymbol{\xi} - \boldsymbol{x}) \, d\Omega_\xi}_{= g(\boldsymbol{y}, \boldsymbol{x})} \\ &= \int_\Gamma g(\boldsymbol{\xi}, \boldsymbol{y}) \frac{\partial G}{\partial n}(\boldsymbol{\xi}, \boldsymbol{x}) \, ds_\xi + g(\boldsymbol{y}, \boldsymbol{x}) \, . \end{aligned} \tag{6.23}$$

Next, we repeat this with the FE-approximation $G_h(\boldsymbol{y}, \boldsymbol{x})$, which is the solution to the boundary value problem

$$-\Delta G_h(\boldsymbol{y}, \boldsymbol{x}) = \delta_h(\boldsymbol{y}, \boldsymbol{x}) \qquad G_h = 0 \qquad \text{at the edge } \Gamma \, , \tag{6.24}$$

where $\delta_h(\boldsymbol{y}, \boldsymbol{x})$ is a patchwork of distributed forces (and line forces), which try to simulate the action of a true point load, of a Dirac delta $\delta(\boldsymbol{y} - \boldsymbol{x})$. Therefore $G_h(\boldsymbol{y}, \boldsymbol{x})$ has the integral representation

$$G_h(\boldsymbol{y}, \boldsymbol{x}) = \int_\Gamma g(\boldsymbol{\xi}, \boldsymbol{y}) \underset{\uparrow}{\frac{\partial G_h}{\partial n}}(\boldsymbol{\xi}, \boldsymbol{x}) \, ds_\xi + \int_\Omega g(\boldsymbol{\xi}, \boldsymbol{y}) \, \delta_h(\boldsymbol{\xi}, \boldsymbol{x}) \, d\Omega_\xi \, , \tag{6.25}$$

and here we see the critical point. At the re-entrant corner **the slope** $\partial G_h / \partial n$ of the membrane will probably be infinite (we are talking now about the load case $\delta_h(\boldsymbol{y}, \boldsymbol{x})$) and such singular shapes cannot be modeled accurately with finite elements, which means the normal derivative $\partial G_h / \partial n$ of the FE-solution will be inaccurate at the corner, and because this inaccuracy affects, see (6.25), also $G_h(\boldsymbol{y}, \boldsymbol{x})$, the influence function $G_h(\boldsymbol{y}, \boldsymbol{x})$ will be less accurate—not only at the corner—but in the whole domain, at any point.

Singularities on the edge propagate through this mechanism into the interior and reduce the quality of the influence function and therefore of the FE-solution w_h itself.

$$\frac{\partial G}{\partial n} \quad \rightarrow \quad \frac{\partial G_h}{\partial n} \quad \rightarrow \quad G_h \quad \rightarrow \quad w_h = \int_\Omega G_h \, p \, d\Omega_y$$

Nothing can break this chain.

This is like a canvas throwing wrinkles when the suspension on the edge is faulty.

To be precise we would have to add to the domain integral in (6.25) also the contributions of the line loads l_h (= jumps in the slope of $G_h(\boldsymbol{y}, \boldsymbol{x})$)

$$\int_{\Omega} g(\boldsymbol{\xi}, \boldsymbol{y})\, \delta_h(\boldsymbol{\xi}, \boldsymbol{x})\, d\Omega_{\xi} + \sum_i \int_{\Gamma_i} g(\boldsymbol{\xi}, \boldsymbol{y})\, l_h(\boldsymbol{\xi}, \boldsymbol{x})\, ds_{\xi}\,, \tag{6.26}$$

but we read the domain integral in (6.25) as a shorthand for both contributions. Here the focus is on the slope on the boundary and its effect. ***The slope is the critical part***.

Wall Plates

What in a membrane is the slope, are the tractions $\boldsymbol{t} = \boldsymbol{S}\,\boldsymbol{n}$ on the edge of a plate, and the equation analogous to (6.21) is the integral representation (*in tensor notation, summation over repeated indices is implied*)

$$u_i(\boldsymbol{x}) = \int_{\Gamma} (G^F_{ij}(\boldsymbol{y}, \boldsymbol{x})\, t_j(\boldsymbol{y}) - T^F_{ij}(\boldsymbol{y}, \boldsymbol{x})\, u_j(\boldsymbol{y}))\, ds_y + \int_{\Omega} G^F_{ij}(\boldsymbol{y}, \boldsymbol{x})\, p_j(\boldsymbol{y})\, d\Omega_y$$

of a displacement field $\boldsymbol{u}(\boldsymbol{x}) = \{u_1, u_2\}^T$.

The functions $G^F_{ij}(\boldsymbol{y}, \boldsymbol{x})$ are the displacements ($j = 1, 2$) (x- and y-direction) of the elastic plane of infinite extent, if a single force $P = 1$ pushes the node $\boldsymbol{x}$ into the directions $i = 1, 2$ and the functions $T^F_{ij}(\boldsymbol{y}, \boldsymbol{x})$ are the tractions ($j = 1, 2$) (x- and y-direction) of these fields on the curve Γ.

The 2×2 matrix $\boldsymbol{G}^F$ is called the ***Somigliana matrix***, and it plays the same role as the function $g(\boldsymbol{y}, \boldsymbol{x})$ in (3.41), since it is the fundamental solution of the governing 2×2 system of equations (7.27).

When we apply this integral representation to Green's function this leads to

$$\begin{aligned} G_{ij}(\boldsymbol{y}, \boldsymbol{x}) = &\int_{\Gamma} (G^F_{jk}(\boldsymbol{\xi}, \boldsymbol{y})\, T_{ik}(\boldsymbol{\xi}, \boldsymbol{x}) - T^F_{jk}(\boldsymbol{\xi}, \boldsymbol{y})\, G_{ik}(\boldsymbol{\xi}, \boldsymbol{x}))\, ds_{\xi} \\ &+ \int_{\Omega} G^F_{jk}(\boldsymbol{\xi}, \boldsymbol{y})\, \delta_{ik}(\boldsymbol{\xi} - \boldsymbol{x})\, d\Omega_{\xi}\,, \end{aligned} \tag{6.27}$$

and in the case of the FE-solution to

$$\begin{aligned} G^h_{ij}(\boldsymbol{y}, \boldsymbol{x}) = &\int_{\Gamma} (G^F_{jk}(\boldsymbol{\xi}, \boldsymbol{y})\, \underset{\uparrow}{T^h_{ik}}(\boldsymbol{\xi}, \boldsymbol{x}) - T^F_{jk}(\boldsymbol{\xi}, \boldsymbol{y})\, G^h_{ik}(\boldsymbol{\xi}, \boldsymbol{x}))\, ds_{\xi} \\ &+ \int_{\Omega} G^F_{jk}(\boldsymbol{\xi}, \boldsymbol{y})\, \delta^h_{ik}(\boldsymbol{\xi}, \boldsymbol{x})\, d\Omega_{\xi}\,. \end{aligned} \tag{6.28}$$

This suffices to recognize that the sensitive part in the approximation of the FE-influence function $G_{ij}^h(\boldsymbol{y}, \boldsymbol{x})$ are **the tractions** T_{ik}^h due to the approximate point load, the Dirac delta δ_{ik}^h. At singular points on the boundary the accuracy of these tractions will be questionable.

Kirchhoff Plates

What in a membrane is the slope are the moments and the Kirchhoff shear (support reactions) along the edge of the plate. Their singularities have a decisive influence on the accuracy of the FE-influence functions, see Fig. 6.22. In very simplified terms does the influence function of a plate look like,

$$w(\boldsymbol{x}) = \int_\Gamma (g\, w''' + g' w'' + g'' w' + g''' w)\, ds_{\boldsymbol{y}} + \int_\Omega g\, p\, d\Omega_{\boldsymbol{y}}\,, \tag{6.29}$$

where

$$g(\boldsymbol{y}, \boldsymbol{x}) = \frac{1}{2\,\pi\, K}\, r^2\, \ln r \qquad K = \frac{E\, h^3}{12\,(1-\nu^2)} \tag{6.30}$$

is the fundamental solution, and K is the plate stiffness.

In this notation w' is the slope on the boundary, w'' is the moment and w''' is the Kirchhoff shear. The exact influence function G has the boundary values $G = 0$ and $G'' = 0$ (hinged edge), and so the formula reduces to

$$G(\boldsymbol{y}, \boldsymbol{x}) = \int_\Gamma (g\, G''' + g''\, G')\, ds_{\boldsymbol{y}} + g(\boldsymbol{y}, \boldsymbol{x})\,. \tag{6.31}$$

The FE-influence function satisfies the zero-moment condition $G'' = 0$ on the hinged edge only approximately, and so we are not allowed to drop its contribution

$$G_h(\boldsymbol{y}, \boldsymbol{x}) = \int_\Gamma (g\, G_h''' + g' G_h'' + g'' G_h')\, ds_{\boldsymbol{y}} + \int_\Omega g\, \delta_h\, d\Omega_{\boldsymbol{y}}\,. \tag{6.32}$$

Consequently, the quality of the FE-influence function depends on the slope G_h' and the moment

$$G_h'' \equiv m_{xx}\, n_x^2 + 2\, m_{xy}\, n_x\, n_y + m_{yy}\, n_y^2 \qquad \text{(2nd deriv.)} \tag{6.33}$$

and the shear force

$$G_h''' \equiv m_{ij,j}\; n_i + \frac{d}{ds}\, m_{nt} \qquad \text{(3rd deriv.)}\,. \tag{6.34}$$

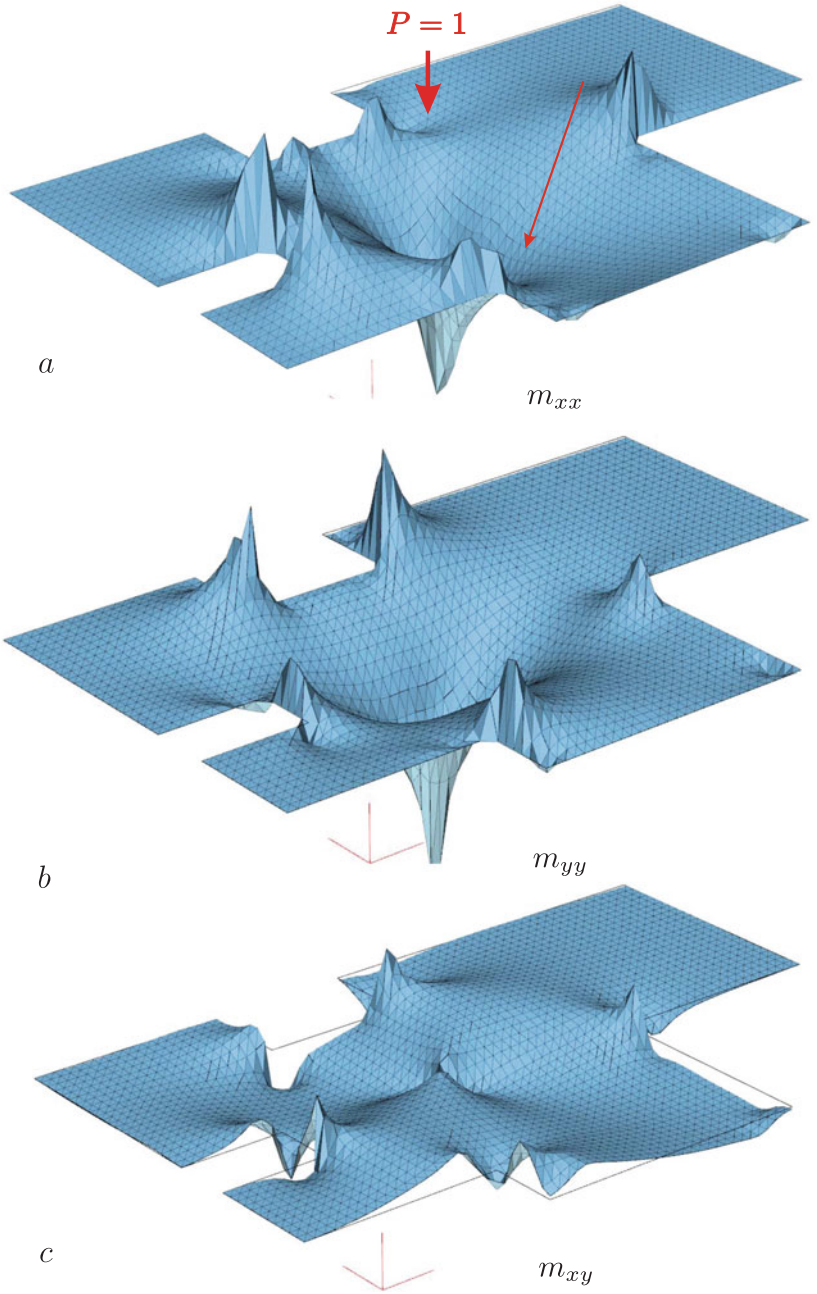

Fig. 6.22 Hinged plate and the bending moments produced by the Dirac delta $P = 1$, which generates the influence function $G_0(\boldsymbol{y}, \boldsymbol{x})$ for the deflection $w(\boldsymbol{x})$. At reentrant corners the moments become singular and this has a negative effect on the quality of the FE-influence function

If these functions are critical at a corner point, it will obviously diminish the quality of the influence function.

All this applies to the influence functions of the internal forces as well

$$m_{xx}(\boldsymbol{x}) = \int_\Gamma (G_2\, w''' + \cdots \qquad v_x(\boldsymbol{x}) = \int_\Gamma (G_3\, w''' + \cdots \tag{6.35}$$

and these react even more sensitively to singularities since they calculate second- or third-order derivatives. This is better seen, if we write (6.29) for all four quantities w, w', w'', w''' and keep only the **characteristic singularities** of the kernels

$$\begin{bmatrix} w \\ w' \\ w'' \\ w''' \end{bmatrix} = \int_\Gamma \begin{bmatrix} \boxed{r^{-1}} & \ln r & r \ln r & r^2 \ln r \\ r^{-2} & \boxed{r^{-1}} & \ln r & r \ln r \\ r^{-3} & r^{-2} & \boxed{r^{-1}} & \ln r \\ r^{-4} & r^{-3} & r^{-2} & \boxed{r^{-1}} \end{bmatrix} \begin{bmatrix} w \\ w' \\ w'' \\ w''' \end{bmatrix} ds_y + \int_\Omega \begin{bmatrix} G_0 \\ G_1 \\ G_2 \\ G_3 \end{bmatrix} p\, d\Omega_y\,. \tag{6.36}$$

Column #1 is the Kirchhoff shear of the G_i, column #2 are the moments, next come the normal derivatives and finally, in column #4, the G_i itself.

So much for the theory. In practice, however, the effects of singularities are unlikely to be so dramatic, since engineering accuracy is not that demanding, and the experienced engineer has a well-developed sense of what is credible and what is not.

Finite elements in structural analysis are both, modeling and "slide rule", and the engineer is therefore very flexible—not to say: indulgent—in the interpretation of FE-results.

In the case of the wall plate in Fig. 6.20 the tensile stress at the bottom increased from $\sigma_{xx} = 168$ kN/m^2 to $\sigma_{xx} = 220$ kN/m^2 after an adaptive refinement, see Fig. 6.23, which is an unusually large increase. Not in all cases will the difference be so large; unfortunately, no fixed rules can be established.

We think stress peaks are "harmless", if the plastic zone, which may form, does not cause massive compensating motions. In the case of the wall plate in Fig. 6.23 it is probably different, since it is only held fixed by two "tiny" point supports.

Perhaps a word about the separate roles of finite elements in mathematics and in engineering is in order here. For a mathematician finite elements are functions, shape functions, while for an engineer finite elements are structural elements, and the engineer therefore is not only interested in the approximation error, but also in the **modeling error**.

Both errors are interrelated. In contrast to the construction of a house, finite elements need to improve the foundations, when the roof truss is already in place, and the model still is open to adjustments. The analysis of the modeling error is as impor-